Xingying Huang,[1] Paul A. Ullrich,[1]

1. Introduction

Over past decades, human behaviors have strongly impacted the climate both globally and regionally, mainly through increasing greenhouse gases [*Solomon*, 2007]. Another important factor is land cover change, such as deforestation and urbanization [*Bonan*, 1997; *Pielke et al.*, 2002; *Kueppers et al.*, 2008]. Due to the expansion of the human population, conversion of natural land surface to cropland is prominent, resulting albedo and net radiation changes including both sensible and latent heat fluxes (foley2003green). Additionally, except the cropland itself, the land management also plays a important role in affecting the climate by modifying the carbon and water cycles, such as different cropping length and irrigation strategy (lobell2006biogeophysical). The cooling effect by irrigation, especially over some extensively irrigated areas, has already been shown in previous studies [*Kueppers et al.*, 2007; *Lobell and Bonfils*, 2008].

California is the topmost irrigating state in the United States, and most of California's irrigated cropland is distributed over the Central Valley (CV), producing 25% of the agricultural products in the U.S. [*Wilkinson et al.*, 2002]. CV, ranging nearly 600 km from north to south and 60-100 km from west to east, is known by its vast agricultural industry and in contrast the extremely dry growing seasons under the Mediterranean climate. The USGS reported that in year 2000, about 42 km^3 of water is used over 41,000 km^2 of irrigated area in California [*Döll and Siebert*, 2002; *Famiglietti et al.*, 2011]. *Bonfils and Lobell* [2007] found that irrigation over CV has decreased summertime maximum temperature by ∼2-3 K in heavily-irrigated areas compared with nearby non-irrigated areas, based on long-term temperature records, and stated that irrigation has negligible effects on nighttime temperatures. Similar results have also been shown in Nebraska's irrigated areas by [*Mahmood et al.*, 2006].

However, irrigation effects are usually ignored in climate modeling due to multiple reasons including its small area (∼2% of global land surface) and its seeming negligible cooling effect compared to global greenhouse warming [*Boucher et al.*, 2004]. However, with the increasing need for more accurate regional climate studies, irrigation practice could be a important factor regulating heavy irrigated area's climate patterns. For this purpose, climatic effects of irrigation have been modeled mainly by limited-area models (LAMs) (or referred as regional climate models (RCMs)) [*Snyder et al.*, 2006; *Kueppers et al.*, 2007]. Irrigation was modeled differently among those studies including when the irrigation is needed, how much irrigated water will be added and the area of cropland that will be irrigated. *Kueppers et al.* [2007], using RegCM3 (the third generation of the Regional Climate Model), simulated the effect of irrigation on regional climate in the Central Valley, California, by forcing the RegCM3 root zone (top 1 m) soil moisture to field capacity at every time step during the simulation period. And they found that the irrigated areas has been cooled by ∼3.7 K in August, through conversion of natural vegetation to irrigated crops. Therefore, the magnitude of the irrigation cooling effect is not only related with the specific land surface model but also controlled by the way irrigation works.

Although global climate models (GCMs) are rarely used to account for irrigation effect, it is meaningful to find out to what extent the irrigation may affect the global climate patterns. *Lobell et al.* [2006] coupled the community atmosphere model (CAM) 3.0 to the community land model (CLM) 3.0 at ∼2-2.5° horizontal grid space to model irrigation by fixing soil moisture at saturation during the growing season in all croplands. And the results showed that irrigation caused a global land surface cooling of 1.3 K, and regional cooling of up to 8 K. *Lo and Famiglietti* [2013] used the CAM 3.5 combined with the CLM 3.5 at ∼1.4°, and showed that the increase in evapotranspiration and water vapor due to irrigation significantly impacts the atmospheric circulation in the southwestern United States with a anthropogenic loop in the regional hydrological cycle.

Aforementioned studies, that worked on the irrigation effect over California, either used RCMs or GCMs at coarse resolution with different irrigation schemes. In order to model regional climate over CV, relatively fine horizontal resolution is needed for a more accurate representation of microclimates, land-use, small-scale dynamical features and interactions and to provide more useful info for formulating climate adaptation and mitigation strategies [*Leung et al.*, 2003; *Rauscher et al.*, 2010]. In this paper, we use the recently developed variable-resolution option in Community Earth System Model (VR-CESM) as our GCM to study the impact of irrigation on regional climate over CV in California, under a more flexible irrigation scheme with relatively realistic estimates of regional agricultural water use (as described in Section 2). VR-CESM is one type of variable-resolution GCM (VRGCM), which uses a relatively coarse global model with enhanced resolution over a specific region [*Staniforth and Mitchell*, 1978; *Fox-Rabinovitz et al.*, 1997]. Compared with RCMs, a key advantage of VRGCMs is that they use a single, unified modeling framework, rather than separate GCM and RCM with potentially inconsistent dynamics and physics parameterizations and lack of two-way interactions at the nest boundary [*Laprise et al.*, 2008]. Compared to uniform-resolution global models, VRGCMs provide a cost-effective method of reaching high resolutions over a region of interest – the limited area simulations in this study at ∼28 km resolution represent a reduction in required computation of approximately 10 times. VR-CESM have been demonstrated to be effective for regional climate studies and applications at a reduced computational cost compared to uniform GCMs [*Zarzycki et al.*, 2015; *Rhoades et al.*, 2015].

The study applied the irrigation option in CLM 4.0 coupled in CESM 1.2.0 to investigate the impact of irrigation not only on mean climatology, but also on heat extremes over recently past climate from year 1980-01-01 to 2005-12-31 in CV. This paper is organized as follows. Section 2 describes the model setup, employed datasets and methodology. In section 3, simulation results are provided and discussed. Key results are summarized along with further discussion in section 4.

[1]Department of Land, Air and Water Resources, University of California, Davis

0094-8276/15/$5.00

2. Model setup and reference datasets

2.1. Irrigation scheme

As a state-of-the-art Earth modeling framework, CESM consists of coupled atmospheric, oceanic, land and sea ice models [*Neale et al.*, 2010a; *Hurrell et al.*, 2013]. In this study, CAM version 5 (CAM5) [*Neale et al.*, 2010b] and the Community Land Model (CLM) version 4.0 [*Oleson et al.*, 2010a] are used. The finest horizontal resolution of our grid is 0.25 ° (∼ 28km) covering the western U.S., with a quasi-uniform 1 ° mesh over the remainder of the globe. Detailed descriptions of VR-CESM employed in this paper can be found in *Rhoades et al.* [2015], here, we only focus on the irrigation scheme within CLM 4.0.

The irrigation modeling is implemented by applying a relatively realistic amount of irrigation water based on leaf area index (LAI) and explicitly calculate the effects on the surface water and energy balance, mostly like the way stated in [*Sacks et al.*, 2009]. The fraction area of the cropland (independent of specific type) that equipped for irrigation is from *Siebert et al.* [2005, 2007] matching year 2000, and is fixed over the simulation period (see Figure 1). This is still reasonable since irrigated area has become stable in California since 1980 as stated in*Bonfils and Lobell* [2007].

The need of irrigation is checked at 6 AM local time by computing the deficit between the current soil moisture content and a target soil moisture content. The calculated deficit is the amount of water that will be added through irrigation if it is positive. Then, irrigation is applied at a constant rate over the following four hours and is directly added to the ground surface bypassing canopy interception. The target soil moisture content in each soil layer i ($w_{target,i}$, kg/m^2) is a weighted average of (a) the minimum soil moisture content that results in no water stress in that layer ($w_{o,i}$, kg/m^2) and (b) the soil moisture content at saturation in that layer ($w_{sat,i}$, kg/m^2) (as the Equation (1)) [*Oleson et al.*, 2010b]. There are ten soil layers with a total depth of 3.4 m [*Oleson et al.*, 2010b]. The default value of the irrigation weight factor α is 0.7, which was determined empirically to give global, annual irrigation amounts that approximately match observed gross irrigation water use around the year 2000 [*Shiklomanov*, 2000]. More details about the way that the irrigation works in CLM 4.0 can be found from the on-line technical descriptions (`http://www.cesm.ucar.edu/models/cesm1.2/clm/`).

$$w_{target,i} = (1 - \alpha) * w_{o,i} + \alpha * w_{sat,i} \qquad (1)$$

2.2. Simulations

In order to understand the climate effects caused by irrigation, we have conducted a control run (named NRG) without irrigation and two irrigation-enabled runs, called IRG and IRG(0.5) respectively. The only difference between the two irrigation runs is that instead of using the default irrigation weight factor α of 0.7 as IRG, we adjusted the α to 0.5 in the IRG(0.5) run, to figure out whether and how different amounts of irrigated water can impact our results. Those three long-term simulations were performed over the time period from 1979-01-02 to 2005-12-31 (UTC) and 1979 is discarded as a spin-up period. This time period was chosen to provide an adequate sampling of annual variability, and to limit computational cost.

For NRG run, we used the land cover dataset at 0.5 ° fixed at year 2000. After this run, we found that there is another available land cover dataset at 3min(∼10 km) resolution in year 2000, which produced more realistic fraction of irrigated cropland at each grid cell over CV. Thus, we used that higher resolution for our irrigation runs. The land cover datasets are interpolated to our grid resolutions during the simulation.

3. Methodology

Irrigation practice peaks in summer growing season [*Salas et al.*, 2006], since there is rarely precipitation (add observation values here) and the land surface is extremely dry. Similarly, for the model, most irrigated water is added during summer (see supplement document for further info). Together with the extreme hot summer in CV, irrigation effects can be best studied over summer. Therefore, we focus on June, July and August (JJA) for assessment of near surface temperature changes caused by irrigation and the relevant mechanisms. Specifically, our results analysis focuses on daily maximum, minimum and average 2m temperatures (T_{max}, T_{min} and T_{avg}).

We did not de-trend the datasets since the linear trend is too small. To restrict the analysis in our study region CV, relevant variables of the simulations and datasets have been masked under the boundary showed in Figure 1 containing 155 grid cells.

add info for supplement: Complementary results to this study are provided in the online supplement, including the xxx.

3.1. Reference datasets

Two gridded observational datasets of the highest available quality and selected weather stations datasets are employed to evaluate our simulation output. The detailed descriptions of these reference datasets are as follows.

UW: The UW daily gridded meteorological data is obtained from the Surface Water Modeling group at the University of Washington [*Maurer et al.*, 2002; *Hamlet and Lettenmaier*, 2005]. The dataset is provided at 0.125° horizontal resolution covering the period from year 1949 to 2010 with daily time frequency. We used UW's T_{max} and T_{min} datasets.

PRISM: The Parameter-elevation Regressions on Independent Slopes Model (PRISM) [*Daly et al.*, 2008] supports a 4 km gridded dataset obtained by taking point measurements and applying a weighted regression scheme that accounts for many factors affecting the local climatology. PRISM is the United States Department of Agriculture's official climatological dataset. Monthly climatological variables are available for 1895 through 2015, and daily dataset are available for 1981 to 2015, from the PRISM Climate Group (Oregon State University, `http://prism.oregonstate.edu`, created 4 Feb 2004). Here, we used both monthly dataset of T_{max}, T_{min} and T_{avg}, and daily dataset of T_{max}.

NCDC: Recorded weather station measurements over the CV are obtained from Global Historical Climate Network, provided by the NOAA/NCDC, `http://www.ncdc.noaa.gov/`). We tried to select the weather stations that distribute evenly over our study region, and satisfy the criterion that at least 90% observations of T_{max} and T_{min} are available over the days of JJAs from 1980 to 2005. At last, ∼20 weather stations observations are used for T_{max} and T_{min}.

4. results

The average JJA T_{min}, T_{avg} and T_{max} over 1980-2005 time period of all the simulations and observational datasets are showed in Figure 2. It can been that NRG has prominent overestimation for T_{max}, with MSD values of ~1 K and RMSD values of ~1.8 K (see Table 1). The cooling effect caused by irrigation in IRG, as previous studies showed, can be clear seen from the aforementioned figure, though no notable difference is observed after reducing the irrigation factor from 0.7 to 0.5. However, the IRG run has overcooling effect with MSD of ~ -0.36 K, and the less irrigated run slightly reduce the underestimation to ~ -0.2 K. Comparing with NRG, the RMSD values of irrigation runs only reduced for about 20%, which may due to the offset effects caused by the non-irrigated grid cells around our study region's boundary. T_{min}s are almost the same for all these runs, being generally warmer comparing with UW and PRISM. Thus, comparing with PRISM, the NRG run overestimated T_{avg} over CV, except the area that strongly impacted by the delta sea breeze. And IRG displayed overall underestimation of T_{avg} due to the overcooled effect. Over the non-irrigated area, the results are almost the same for all the runs, and this further supports our conclusions of the climate effects caused by irrigation. UW and PRISM are statistically the same in T_{max}, proving the consistency between these two observations.

In order to further figure out the potential underlying processes related with irrigation, we have looked into multiple relevant variables as summed in Table 2. Under irrigation, the specific humidity has increased about 15% and the sensible heat flux has decreased 16% mainly along with the cooler surface. Due to the scarcity of precipitation (~0.1 mm/day) and extreme hot summer over CV, the latent heat flux has largely increased for about 71% after adding ~0.2 mm/day irrigated water for IRG(0.5), as further shown in Figure 3. Ground evaporation is positively related with latent heat flux. The average soil moisture over all the subsurface layers has only increased a little (~ 5%) under irrigation (also see Figure 3). Although the irrigated water of IRG(0.5) is nearly half of what for IRG, they did not show notable differences for those variables, which explains the similar results of the near surface temperatures from these two irrigation runs as we discussed above. The possible reason may due to abnormally large surface runoff (~1.6 mm/day) for IRG0.7 comparing with IRG0.5 (~0.24 mm/day) ???.

We have also investigated the relationships among relevant variables based on the JJA values over 26 years to see if the land surface model works reasonably with irrigation. It turned out that, for IRG(0.5) irrigated water is positively correlated with soil moisture, however, this does not hold for IRG. And latent heat flux is positively correlated with soil moisture especially for IRG(0.5) and NRG. T_{max} is positively correlated with irrigated water for in IRG(0.5) run but not correlated with soil moisture or latent heat flux. (add correlation coefficients here??) The boxplot in Figure 3 showed that both the average magnitude and variability of T_{max} has been improved with irrigation. Though average precipitation did not differ among these three runs, adding irrigation tends to widen the distribution of precipitation intensity and bring more extreme precipitation occurrences.

Since hot spells dominate during the summer season over CV, the frequency distribution of T_{max} using all JJA daily values at each grid point over year 1981-2005 is depicted for all the runs and reference datasets including UW, PRISM and xx?? numbers of weather stations in Figure 4. As we can see, compared with NRG, irrigation runs displayed much closer distribution to UW and PRISM, especially over the upper bound, though some colder bias is existed between lower bound and upper bound. The NRG run exhibited a clear warm bias associated with a long forward upper tail with maximum temperatures approaching near 50 °C. Overall, though irrigation runs captures the general distribution of T_{max}, they are not so skewed to left and have more flat peaks than observations as told by the moments in Table 3.

Due to the important role CV plays in agricultural industry, we have also looked at the heat stress for crops. We calculated the hours that exceeding a threshold over each day of JJA based on the hourly outputs from year 2000 (only this year has hourly output) and averaged the value over CV area. Here we chose 35 °C to be our threshold as used in *Teixeira et al.* [2013]. As Figure 5 showed, both the heat stress intensity and frequency have reduced under irrigation. The average hours over all days in this JJA are 2.152 for NRG and 1.424 for IRG (about 34% less).

5. Discussion and Summary

With irrigation, the nighttime warming can occur and daily T_{min} can increase due to the increased thermal conductivity of wet soil found by *Kanamaru and Kanamitsu* [2008], or with increased heat capacity of the soil and vegetation as argued by *Bonfils and Lobell* [2007], over CV. However, in our irrigation runs, T_{min} did not really change, since the soil moisture only increased for about 5% comparing with non-irrigated one and did not result in notable nighttime warming.

Lo and Famiglietti [2013] found that the irrigation in the Central Valley results in higher precipitation rates (~15%) over the southwestern U.S., together with enhancing summer monsoon rainfall. In our study, the specific humidity do increased for about 15% over irrigated area, and this increase also occurred over southern California (see Figure 6) (updated the specific humidity plots over WUS), though, precipitation did not really enlarge (for about %10) (this may due to legend) as *Lo and Famiglietti* [2013] identified in a model. This gives evidence that irrigation in the Central Valley could change the regional hydrological cycle with water vapor transport, as

drip irrigation or flood irrigation

impact for future projections

why only JJA: extra water will be run off rather than soil moisture or latent heat flux

The IRG0.5 and IRG0.7

irrigation water: kern County (CA): area 8140.964496 sq. mile., irrigated water 3.0 km cubic per year (year 2000), http://www.ssjid.com/district-services/agriculture-irrigation-water.htm: Irrigation season runs from approximately March 15 to October 15, depending on the weather and water supplies.

Acknowledgments.

References

Bonan, G. B. (1997), Effects of land use on the climate of the united states, *Climatic Change*, *37*(3), 449–486.

Bonfils, C., and D. Lobell (2007), Empirical evidence for a recent slowdown in irrigation-induced cooling, *Proceedings of the National Academy of Sciences*, *104*(34), 13,582–13,587.

Boucher, O., G. Myhre, and A. Myhre (2004), Direct human influence of irrigation on atmospheric water vapour and climate, *Climate Dynamics*, *22*(6-7), 597–603.

Daly, C., M. Halbleib, J. I. Smith, W. P. Gibson, M. K. Doggett, G. H. Taylor, J. Curtis, and P. P. Pasteris (2008), Physiographically sensitive mapping of climatological temperature and precipitation across the conterminous United States, *International Journal of Climatology*, *28*(15), 2031–2064.

Döll, P., and S. Siebert (2002), Global modeling of irrigation water requirements, *Water Resources Research*, *38*(4), 8–1.

Famiglietti, J., M. Lo, S. Ho, J. Bethune, K. Anderson, T. Syed, S. Swenson, C. de Linage, and M. Rodell (2011), Satellites measure recent rates of groundwater depletion in california's central valley, *Geophysical Research Letters*, *38*(3).

Fox-Rabinovitz, M. S., G. L. Stenchikov, M. J. Suarez, and L. L. Takacs (1997), A finite-difference GCM dynamical core with a variable-resolution stretched grid, *Monthly Weather Review*, *125*(11), 2943–2968.

Hamlet, A. F., and D. P. Lettenmaier (2005), Production of Temporally Consistent Gridded Precipitation and Temperature Fields for the Continental United States*, *Journal of Hydrometeorology*, *6*(3), 330–336.

Hurrell, J. W., M. M. Holland, P. R. Gent, S. Ghan, J. E. Kay, P. Kushner, J.-F. Lamarque, W. G. Large, D. Lawrence, K. Lindsay, et al. (2013), The community earth system model: A framework for collaborative research, *Bulletin of the American Meteorological Society*, *94*(9), 1339–1360.

Kanamaru, H., and M. Kanamitsu (2008), Model diagnosis of nighttime minimum temperature warming during summer due to irrigation in the california central valley, *Journal of Hydrometeorology*, *9*(5), 1061–1072.

Kueppers, L. M., M. A. Snyder, and L. C. Sloan (2007), Irrigation cooling effect: Regional climate forcing by land-use change, *Geophysical Research Letters*, *34*(3).

Kueppers, L. M., M. A. Snyder, L. C. Sloan, D. Cayan, J. Jin, H. Kanamaru, M. Kanamitsu, N. L. Miller, M. Tyree, H. Du, et al. (2008), Seasonal temperature responses to land-use change in the western united states, *Global and Planetary Change*, *60*(3), 250–264.

Laprise, R., R. De Elia, D. Caya, S. Biner, P. Lucas-Picher, E. Diaconescu, M. Leduc, A. Alexandru, and L. Separovic (2008), Challenging some tenets of regional climate modelling, *Meteorology and Atmospheric Physics*, *100*(1-4), 3–22.

Leung, L. R., L. O. Mearns, F. Giorgi, and R. L. Wilby (2003), Regional climate research: needs and opportunities, *Bulletin of the American Meteorological Society*, *84*(1), 89–95.

Lo, M.-H., and J. S. Famiglietti (2013), Irrigation in california's central valley strengthens the southwestern us water cycle, *Geophysical Research Letters*, *40*(2), 301–306.

Lobell, D., G. Bala, and P. Duffy (2006), Biogeophysical impacts of cropland management changes on climate, *Geophysical Research Letters*, *33*(6).

Lobell, D. B., and C. Bonfils (2008), The effect of irrigation on regional temperatures: A spatial and temporal analysis of trends in california, 1934-2002, *Journal of Climate*, *21*(10), 2063–2071.

Mahmood, R., S. A. Foster, T. Keeling, K. G. Hubbard, C. Carlson, and R. Leeper (2006), Impacts of irrigation on 20th century temperature in the northern great plains, *Global and Planetary Change*, *54*(1), 1–18.

Maurer, E., A. Wood, J. Adam, D. Lettenmaier, and B. Nijssen (2002), A long-term hydrologically based dataset of land surface fluxes and states for the conterminous United States*, *Journal of climate*, *15*(22), 3237–3251.

Neale, R. B., C.-C. Chen, A. Gettelman, P. H. Lauritzen, S. Park, D. L. Williamson, A. J. Conley, R. Garcia, D. Kinnison, J.-F. Lamarque, et al. (2010a), Description of the NCAR community atmosphere model (CAM 5.0), *NCAR Tech. Note NCAR/TN-486+ STR*.

Neale, R. B., C.-C. Chen, A. Gettelman, P. H. Lauritzen, S. Park, D. L. Williamson, A. J. Conley, R. Garcia, D. Kinnison, J.-F. Lamarque, D. Marsh, M. Mills, A. K. Smith, S. Tilmes, F. Vitt, P. Cameron-Smith, W. D. Collins, M. J. Iacono, , R. C. Easter, X. Liu, S. J. Ghan, P. J. Rasch, and M. A. Taylor (2010b), Description of the NCAR Community Atmosphere Model (CAM 5.0), *NCAR Technical Note NCAR/TN-486+STR*, National Center for Atmospheric Research, Boulder, Colorado.

Oleson, K., D. Lawrence, G. Bonan, M. Flanner, E. Kluzek, P. Lawrence, S. Levis, S. Swenson, P. Thornton, A. Dai, M. Decker, R. Dickinson, J. Feddema, C. Heald, F. Hoffman, J. Lamarque, N. Mahowald, G. Niu, T. Qian, J. Randerson, S. Running, K. Sakaguchi, A. Slater, R. Stockli, A. Wang, Z. Yang, X. Zeng, and X. Zeng (2010a), Technical description of version 4.0 of the Community Land Model (CLM), *NCAR Technical Note NCAR/TN-478+STR*, National Center for Atmospheric Research, Boulder, Colorado, doi:10.5065/D6FB50WZ.

Oleson, K. W., D. M. Lawrence, B. Gordon, M. G. Flanner, E. Kluzek, J. Peter, S. Levis, S. C. Swenson, E. Thornton, J. Feddema, et al. (2010b), Technical description of version 4.0 of the community land model (clm).

Pielke, R. A., G. Marland, R. A. Betts, T. N. Chase, J. L. Eastman, J. O. Niles, S. W. Running, et al. (2002), The influence of land-use change and landscape dynamics on the climate system: relevance to climate-change policy beyond the radiative effect of greenhouse gases, *Philosophical Transactions of the Royal Society of London A: Mathematical, Physical and Engineering Sciences*, *360*(1797), 1705–1719.

Rauscher, S. A., E. Coppola, C. Piani, and F. Giorgi (2010), Resolution effects on regional climate model simulations of seasonal precipitation over Europe, *Climate Dynamics*, *35*(4), 685–711.

Rhoades, A. M., X. Huang, P. A. Ullrich, and C. M. Zarzycki (2015), Characterizing sierra nevada snowpack using variable-resolution cesm, *Journal of Applied Meteorology and Climatology*, (2015).

Sacks, W. J., B. I. Cook, N. Buenning, S. Levis, and J. H. Helkowski (2009), Effects of global irrigation on the near-surface climate, *Climate Dynamics*, *33*(2-3), 159–175.

Salas, W., P. Green, S. Frolking, and C. Li (2006), Estimating irrigation water use for california agriculture: 1950s to present, *Contract*, *603*, 862–0244.

Shiklomanov, I. A. (2000), Appraisal and assessment of world water resources, *Water international*, *25*(1), 11–32.

Siebert, S., P. Döll, J. Hoogeveen, J.-M. Faures, K. Frenken, and S. Feick (2005), Development and validation of the global map of irrigation areas, *Hydrology and Earth System Sciences Discussions Discussions*, *2*(4), 1299–1327.

Siebert, S., P. Döll, S. Feick, J. Hoogeveen, and K. Frenken (2007), *Global Map of Irrigation Areas*, FAO Frankfurt, Germany.

Snyder, M., L. Kueppers, L. Sloan, D. Cavan, J. Jin, H. Kanamaru, N. Miller, M. Tyree, H. Du, and B. Weare (2006), Regional climate effects of irrigation and urbanization in the western united states: A model intercomparison, *Lawrence Berkeley National Laboratory*.

Solomon, S. (2007), *Climate change 2007-the physical science basis: Working group I contribution to the fourth assessment report of the IPCC*, vol. 4, Cambridge University Press.

Staniforth, A. N., and H. L. Mitchell (1978), A variable-resolution finite-element technique for regional forecasting with the primitive equations, *Monthly Weather Review*, *106*(4), 439–447.

Teixeira, E. I., G. Fischer, H. van Velthuizen, C. Walter, and F. Ewert (2013), Global hot-spots of heat stress on agricultural crops due to climate change, *Agricultural and Forest Meteorology*, *170*, 206–215.

Wilkinson, R., K. Clarke, J. Reichman, and J. Dozier (2002), Preparing for a changing climate: the potential consequences of climate variability and change for california, *Report for the US Global Change Research Program*.

Zarzycki, C. M., C. Jablonowski, D. R. Thatcher, and M. A. Taylor (2015), Effects of localized grid refinement on the general circulation and climatology in the community atmosphere model, *Journal of Climate*, *28*(7), 2777–2803.

Corresponding author: Xingying Huang, Department of Land, Air and Water Resources, University of California Davis, Davis, CA 95616, USA. (xyhuang@ucdavis.edu)

Table 1. RMSE, MSD, Corr between Tmax of models and observations over CV in JJA from 1980-2005.

JJA	UW			PRISM		
	RMSD	MSD	Corr	RMSD	MSD	Corr
VR-CESM IRG(0.7)	1.511	-0.357	0.999	1.422	-0.355	0.999
VR-CESM NRG	1.809	1.003	0.999	1.824	1.005	0.999
VR-CESM IRG(0.5)	1.467	-0.205	0.999	1.383	-0.203	0.999

Table 2. Values of multiple variables over CV in JJA from 1980-2005.

	QREFHT	SHFLX	U10	LHFLX	PRECT	QIRRIG	QOVER	QSOIL	Rnet	SOILLIQ	QVEGE	QVE
VR-CESM IRG	7.852	104.752	2.913	62.574	0.119	0.473	1.610	0.907	176.795	79.439	0.018	1.23
VR-CESM NRG	6.994	123.211	3.061	36.563	0.107	0.000	0.015	0.163	169.424	75.582	0.016	1.08
VR-CESM IRG(0.5)	7.782	105.730	2.926	61.695	0.118	0.212	0.236	0.892	176.728	78.366	0.017	1.22

Table 3. The first four moments of the JJA T_{max} frequency for models and observations over CV. Column titles refer to the Average (Avg), Variance (Var), Skewness (Skew) and Kurtosis (Kurt).

	Avg	Var	Skew	Kurt
IRG	32.374	21.343	-0.505	0.415
NRG	33.735	27.502	-0.417	0.234
IRG(0.5)	32.537	21.125	-0.556	0.632
UW	32.745	22.442	-0.717	0.794
PRISM	32.814	24.007	-0.802	1.120

Notes: If skew >0 [skew <0], the distribution trails off to the right [left]. If kurtosis >0 [<0], a sharper [flatter] peak compared to a normal distribution (leptokurtic and platykurtic, respectively) is expected.

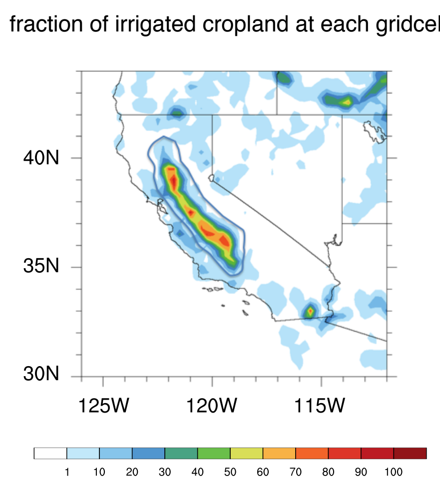

Figure 1. The fraction of irrigated cropland at each grid cell (unit: %). (Blue line is the boundary of the CV region.

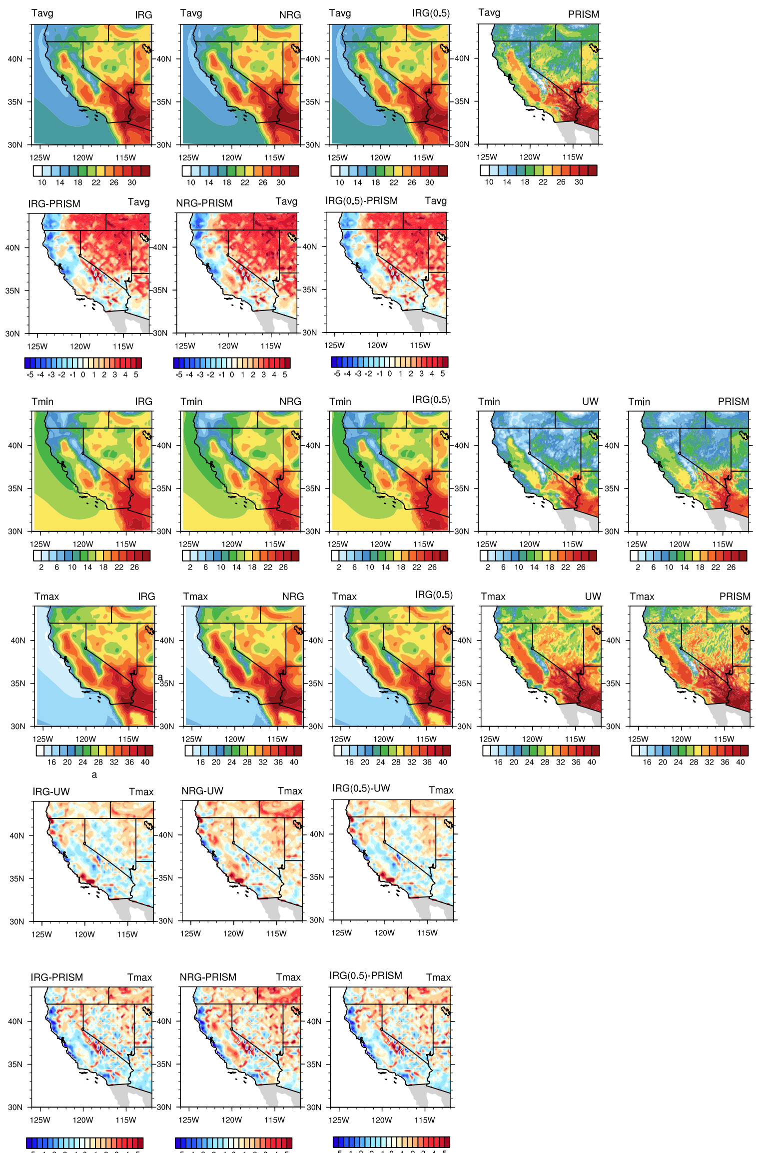
Tavg
IRG
NRG
IRG(0.5)
PRISM
IRG-PRISM
NRG-PRISM
IRG(0.5)-PRISM
Tmin
UW
Tmax
IRG-UW
NRG-UW
IRG(0.5)-UW

Figure 2. .

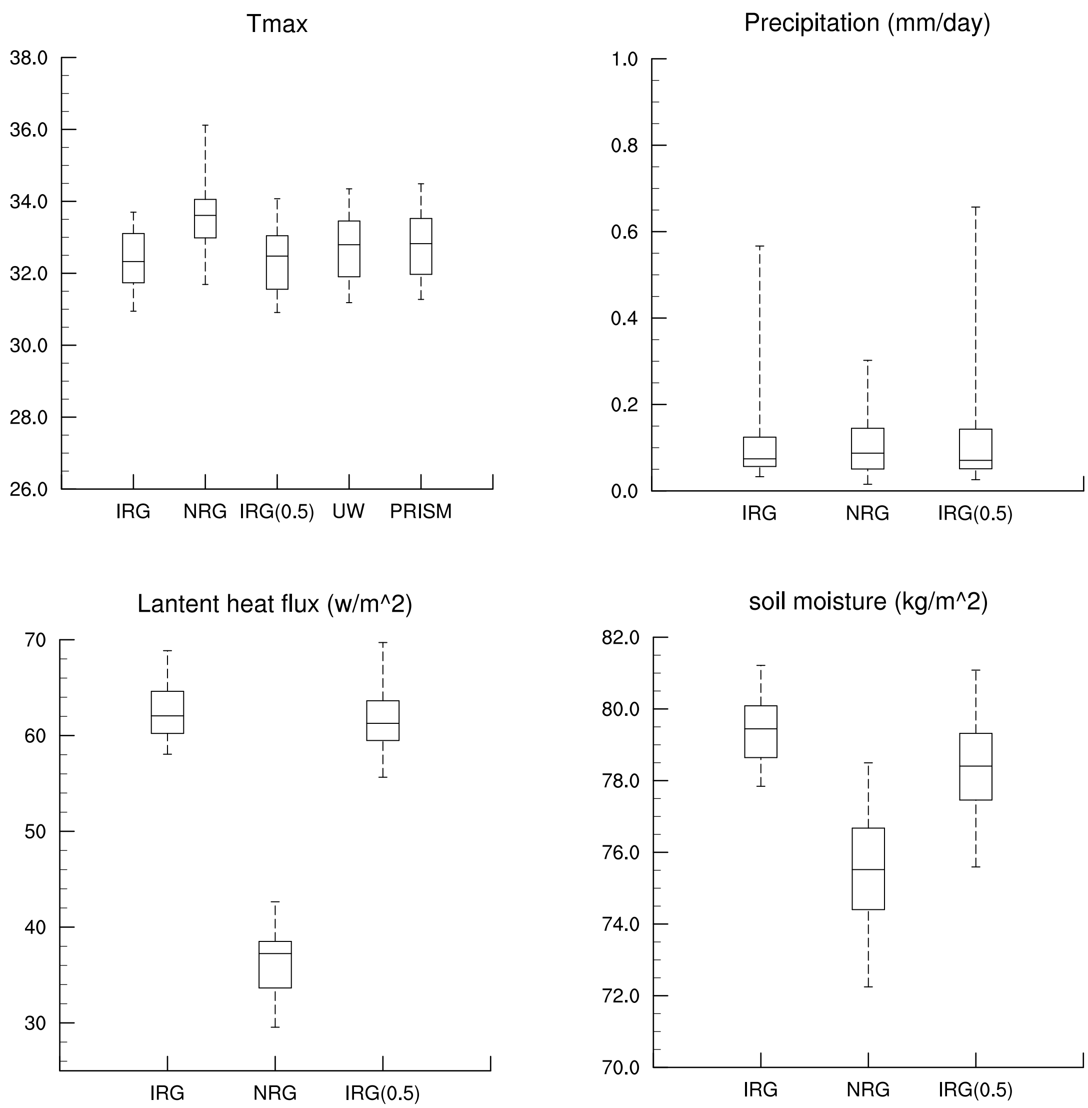
Tmax
38.0
36.0
34.0
32.0
30.0
28.0
26.0
IRG
NRG
IRG(0.5)
UW
PRISM
Precipitation (mm/day)
1.0
0.8
0.6
0.4
0.2
0.0
IRG
NRG
IRG(0.5)
Lantent heat flux (w/m^2)
70
60
50
40
30
IRG
NRG
IRG(0.5)
soil moisture (kg/m^2)
82.0
80.0
78.0
76.0
74.0
72.0
70.0
IRG
NRG
IRG(0.5)

Figure 3. .

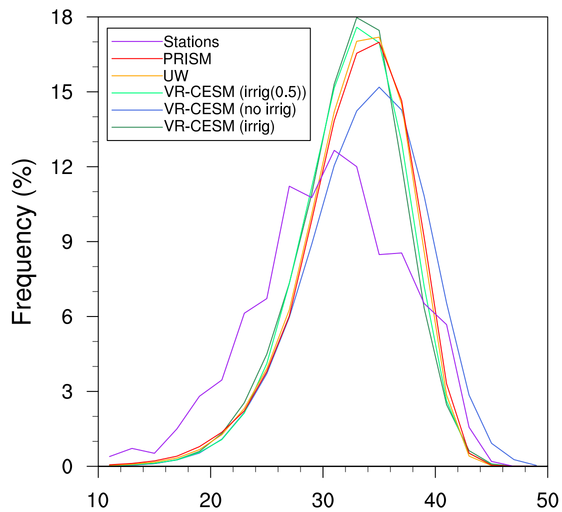

Stations
PRISM
UW
VR-CESM (irrig(0.5))
VR-CESM (no irrig)
VR-CESM (irrig)
Frequency (%)
18
15
12
9
6
3
0
10
20
30
40
50

Figure 4. .

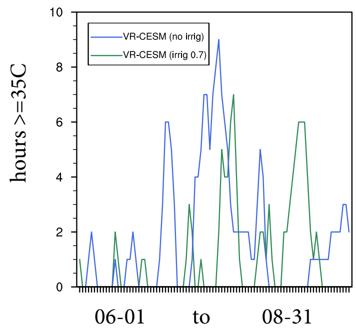
VR-CESM (no irrig)
VR-CESM (irrig 0.7)
hours >=35C
06-01 to 08-31
0
2
4
6
8
10

Figure 5. .

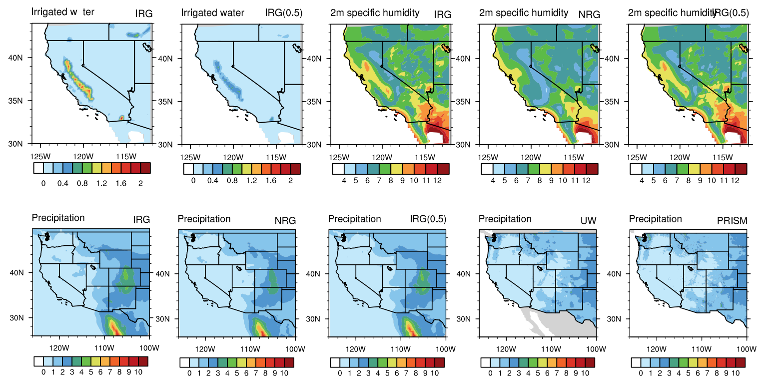
Irrigated w ter
IRG
Irrigated water
IRG(0.5)
2m specific humidity
IRG
2m specific humidity
NRG
2m specific humidity
IRG(0.5)
Precipitation
IRG
Precipitation
NRG
Precipitation
IRG(0.5)
Precipitation
UW
Precipitation
PRISM
40N
35N
30N
125W
120W
115W
110W
100W
0 0.4 0.8 1.2 1.6 2
4 5 6 7 8 9 10 11 12
0 1 2 3 4 5 6 7 8 9 10

a

Figure 6. .